

Nanostructured Insights: Exploring Structural Properties and Characterization Challenges in Clay-Based Hybrid Nanocomposites

¹Bommanna .K*, ²Mohan Kumar .K, ³Kari Ramakrishna, ⁴Shashikumar .T, ⁵Laxmi .B. Wali, ⁶Rajesh Chandra .C, ⁷Anupama .B. Somanakatti, ⁸Hareesh .A

¹Assistant Professor, Department of Mechanical Engineering, APS College of Engineering, Bangalore, Karnataka, India

²Assistant Professor, Department of Mechanical Engineering, MVJ College of Engineering, Bangalore, Karnataka, India

³Assistant Professor, Department of Mechanical Engineering, Amruta Institute of Engineering and Management Sciences, Bidadi, Bangalore, India

⁴Senior Lead Engineer, Collins Aerospace, Advanced Structures-AMTS Group, Bangalore, Karnataka, India

⁵Assistant Professor, Department of Mechanical Engineering, RNS Institute of Technology, Bangalore, Karnataka, India

⁶Assistant Professor, Department of Mechanical Engineering, Dr. Ambedkar Institute of Technology, Bangalore, Karnataka, India

⁷Assistant Professor, Department of Mechanical Engineering, APS College of Engineering, Bangalore, Karnataka, India

⁸Professor, Department of Mechanical Engineering, APS College of Engineering, Bangalore, Karnataka, India

Abstract:- The glass-epoxy hybrid composite is created using a manual lay-up approach with halloysite nanotubular particles. Actually, the direction of nano-clay particles may lead to agglomeration, to overcome this problem the epoxy is needed to be chemically treated. The thermal chemical reaction between epoxy resin and unsaturated polyester was facilitated by an initiator in the form of benzyl peroxide radical. The produced composite was tested using an X-Ray Diffractometer. After that, Halloysite nanotubular (HNT) clay was added in increments of 1, 2, and 3% (by weight) to epoxy and unsaturated polyester toughened epoxy systems. This paper aims to characterize the wear properties of epoxy polymers and glass fiber-reinforced hybrid composites with clay. Characterization is done by using X-Ray Diffraction and performance levels of the composite at different percentage of nano clay addition are observed. Under this study, wear tests of the Pin-on-disc type have been carried out at various loads and times for varying percentage compositions of nano clay particle addition, and the corresponding variations have been investigated.

Keywords: polymer-clay, pin-on-disk, X-ray diffraction, Halloysite nano clay.

1. Introduction

When it comes to creating advanced composites, hardware, electronic circuit boards, radomes, and missile equipment parts, epoxy resin is a very adaptable and esteemed matrix material. This is because of its exceptional bonding qualities in addition to its favourable mechanical, thermal, dielectric, ageing, and physico-chemical properties [1–7].

Meanwhile, because of its nanoscale size and intercalation properties, inorganic hollow-site nanotubes (HNT) clay has become a preferred reinforcement material for many polymers [8].

Cetyltrimethyl ammonium ions are added to the HNT clay to modify it and make it more organophilic in its interaction with the polymer matrix. With the use of cationic surfactants and an ion exchange technique, the clay's surface is modified. Through this method, the clay's surface energy is effectively decreased, improving the compatibility of the clay's surface with the polymer matrix. As a result, adding organophilic HNT clay to epoxy resin helps to make up for any losses that may occur from the lack of strong chemical modifiers like bismaleimide by restoring heat stability and impact strength. As a result, the mechanical and thermal properties of the modified organophilic HNT clay reinforced epoxy nanocomposites are significantly improved. Enhanced barrier qualities, decreased flammability, and longer temperature durability are a few of these advantages [9].

Recently, organic-inorganic nanocomposites have attracted attention. Their remarkable properties and unique structure have led to the synthesis and study of a variety of hybrid composite materials [10]. The intercalation of inorganic materials by organic guest species is a way to construct an ordered organic-inorganic assembly [11]. The high mechanical and thermal qualities of epoxy resins make them the material of choice for matrices. They also have low moisture absorption and good wetting characteristics on a variety of substrate substrates. Epoxy resins also have good electrical qualities and outstanding chemical resistance [12]. Recent study has focused on examining the wear characteristics of polymeric composites with various reinforcements [13]. It has been exhibiting that integrating particles into polymers can reduce the wear rate and coefficient of friction of the resulting composites. Additionally, it has been noted that the mechanical strength and tribological properties of metal-matrix composites are enhanced by the use of SiC as a filler material [14]. The filler is classified as a layered nanomaterial, such as organosilicates, when it has a thickness on the nanoscale scale and a plate-like structure with a high aspect ratio (between 30 and 1000) [15]. Due of their high aspect ratios, nanoparticles provide an overall increased level of reinforcing efficiency [16].

The sizes of a nanocomposite's component phases and the degree of mixing between them greatly influence the material's properties. Notable differences in composite properties can be obtained depending on the components used (nanofibre or layered silicate), the cation exchange capacity, the polymer matrix, and the production technique used [17].

The d_{001} spacing of the changed clay and the degree of hybrid structure formation are determined using the X-ray diffraction (XRD) method [16]. Using a Rigaku D/MAX-2000 X-ray diffractometer with Cu $K\alpha$ radiation ($\lambda = 0.154\text{nm}$) and a scanning rate of $1^\circ/\text{min}$, wide-angle XRD investigations were carried out. The formula for determining the crystallographic spacing "d" is $\lambda = 2d\sin\theta$, as stated by Bragg [17].

The XRD was used to characterize the clay. The 14 \AA layer silicates, namely chlorite, mica, kaolinite, and other layer silicates have been found in the untreated clay Sialupe (39/80). Moreover, feldspars and amphiboles were found. The distinctive kaolinite peak became less intense as the temperature rose to 300°C , and by the time it reached 400°C , nothing was left of it. Metakaolinite is usually formed when kaolinite is heated to a temperature just below 450°C , but in this instance, the longer heating time may cause it to happen at a lower temperature [18, 19].

The scientific field of tribology studies the design, wear, lubrication, and friction of surfaces subjected to relative motion [20]. Layered nanoclay-based polymer nanocomposites have attracted a lot of interest since they exhibit a considerable improvement in physical qualities over pure polymers or traditional composites. These improvements include elevated modulus, heightened strength, toughness, fire retardancy, heat resistance, and decreased gas permeability. Three main types of architectures are possible when layered clay and polymer are combined: (i) phase-separated structure, (ii) intercalated structure, and (iii) exfoliated or delaminated structure, the latter of which yields pure nanocomposites [21]. The suitability of materials for industrial usage in applications involving tribological loading depends on a number of criteria, including wear rate, mechanical load carrying capability, and coefficient of friction. Because polymer-based composite materials have better lubrication and wear qualities and are increasingly required to be stable under increased loads and temperatures, they are the material of choice for tribological applications [22 and 23].

The use of clay improves the mechanical characteristics of glass fiber-reinforced epoxy polymer and epoxy-clay

hybrid composites. Two types of clay are used in the current technique: unmodified MMT clay (UC) and organoclay (OC), which is made from montmorillonite (MMT) that has been treated with alkyl ammonium.

Remarkably, the inclusion of OC enhances the thermal characteristics of epoxy-glass fibre composites more effectively than UC-filled hybrids [24]. This paper investigates the impact of introducing fillers, specifically Halloysite Nano clay particles, on the tribological characteristics and characterization of glass-epoxy composite systems. The research focuses on composites created using the manual lay-up technique. The study examines nanocomposites with different concentrations of nanoclay powder (1%, 2%, and 3%), and epoxy polymer as the matrix phase, using XRD technology. The Scherer formula is considered to compute the crystallite diameters, and X-ray diffractometry showed the phases present in the composite.

By examining the diffraction patterns of 1%, 2%, and 3% nanoclay composites, the effect of adding clay to enhance the mechanical properties of glass fiber-reinforced epoxy-clay hybrid composites and epoxy polymer is assessed. By evaluating the wear rate, the study concentrates on how changes in sliding speed, time, and applied force affect the way polymer nanocomposites wear. Sliding speeds between 640 and 1000 RPM, time intervals between 300 and 900 seconds, and applied weights between 5 and 25 N were all part of the experimental setup. A flat-faced pin was placed in contact with a rotating steel disc to undergo hardening in wear testing. The wear rate rises with higher applied weights, longer times, and faster sliding speeds, according to the results.

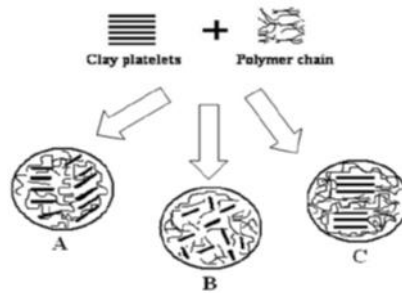


Figure 1: Schematic of the (A) intercalated, (B) exfoliated structure and (C) phase separated polymer-nanoclay composite morphology

2. Methods

Materials used

- The matrix used in this investigation was an epoxy resin system (LY556) combined in a 100:12 ratio with an araldite hardener (HY951) that was purchased from ECMAS Pvt. Ltd., Hyderabad.
- Halloysite nanoclay from Sigma Aldrich, Germany, was used as the reinforcing clay nanoparticle. It was organically changed with 3-aminopropyltriethoxysilane by sonication.
- The supplier of the interwoven roving glass fibre mat was Saint-Gobain-Vetrotex India Ltd.

Synthesis of Composites

Glass fiber-reinforced epoxy-clay hybrids are created by hand-layup techniques that combine glass fibres and resin-clay. The hybrid composite is prepared using a 50% fibre weight and a 50% epoxy resin weight combination. To guarantee thorough curing, the laminates are thereafter cured at room temperature and kept in the mould for a full day.

The process of creating HNT Clay nanocomposites involves mixing treated Halloysite nanoclay particles with hardener and then pouring the mixture into a wooden mould that is 10 mm wide and 100 mm long. Next, the worn specimens are sliced in accordance with the measurements shown in Figure 2.

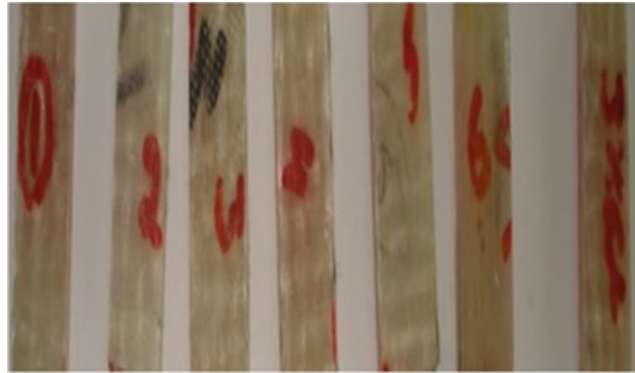


Figure 2: Wear specimens (pure, 1, 2 and 3wt% reinforced Halloysite HNT clay)

Equipment used for Characterization

To investigate the interlayer separation, Research using X-ray diffraction (XRD) were conducted on the epoxy containing clay particles as well as the clay particles alone. The study used CuK α radiation ($\lambda=1.541\text{ \AA}$) running at 30 kV voltage and 15 mA current at a scanning rate of 2° per minute. A Rigaku Ultima IV Model 2036E201 X-ray diffractometer, made in Japan, was used to do the X-ray diffraction.

Using a locally manufactured tribometer, the pin-on-disc wear test was performed in compliance with ASTM G-99 criteria. A loading disc is included in this design to put loads onto square pins. The wear test pins have square diameters of 8 mm and a length of 20 mm. A brass disc was used, and its surface roughness measured 0.21 mm. The test specimens measure 10 mm in width and 100 mm in length. The specific wear rate of both nanocomposites and conventional composites was assessed over a sliding distance of 3600 meters, while keeping a consistent pressure of 0.15 MPa and a sliding velocity of 0.35 m/s.



Figure 3: X-Ray Diffractometer (Model: 2036E201; Rigaku, Ultima IV, Japan)



Figure 4: pin-on-disk set-up (DuCOM, TR-20-M26)

3. Results and Discussions

Characterized by using XRD technique

The XRD technique was employed to fabricate nanocomposites manually, incorporating 1%, 2%, and 3% nanoclay powder with epoxy polymer as the matrix phase, followed by their characterization. Using an X-ray diffractometer, the phases contained in the composite were identified, and the Scherer formula was considered to quantify the diameters of the crystallites. The nanoclay composites' diffraction patterns at 1%, 2%, and 3% concentrations were then contrasted.

Scherer's equation was used to calculate the average crystallite size from the full width at half maximum (FWHM) of the X-Ray diffraction peak. It is simple to compute the crystal size as a function of peak location, peak width (defined as the full width at half maximum peak intensity, or FWHM), and wavelength.

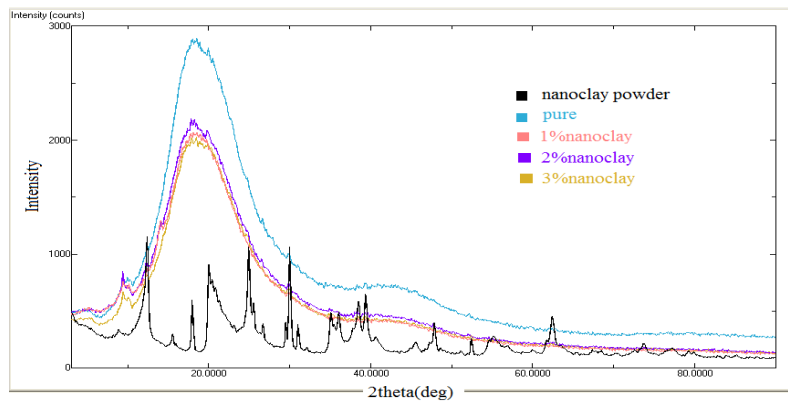


Figure 5: XRD Comparison of Pure Epoxy and Composite Variants

In Figure 5, XRD is used to characterize clay nanopowder in combination with composites that contain 1%, 2%, and 3% nano clay powders, as well as the pure composite with fibre reinforcement. The black diffraction pattern represents the clay nanopowder, whereas the blue plane represents the epoxy polymer composite. Additionally, distinct diffraction patterns are matched by composites reinforced with epoxy polymer fibres containing 1%, 2%, or 3% nano clay powder. The composite that results from spreading the clay nanopowder within the epoxy polymer displays two separate phases: the polymer phase and the particle phase. The particle phase's diffraction pattern resembles that of clay nanopowder, suggesting that it still has a crystalline nature. Conversely, the diffraction patterns of the nanoclay composites at 1%, 2%, and 3% and the pure composite demonstrate the amorphous nature of the epoxy polymers. Tiny peaks that blend into the epoxy diffraction pattern represent the particle phase of the polymer composite.

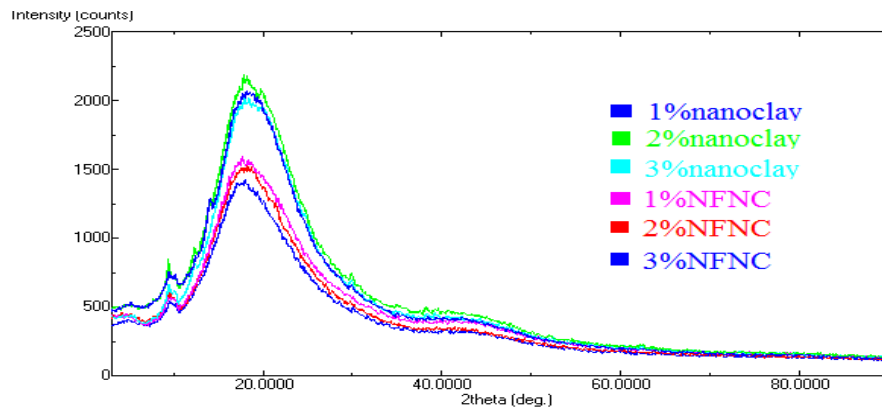


Figure 6: X-ray diffraction patterns of the functionalized and nonfunctional nanoclay composites at 1%, 2%, and 3% Nano Clay powder.

A small diffraction peak at $\theta=9.53$ degrees is seen in all of the diffraction patterns, suggesting that the composite contains clay nanopowder. Furthermore, it seems that the diffraction patterns of the nanoclay composites at 1%, 2%, and 3% and the pure composite are comparable. Fragments of the XRD pattern for each of these phases are compared in Fig. 6, which shows that the pure nanocomposite has a diffraction peak that is 15–20% more intense. On the other hand, compared to the previous phases, the intensity of the clay powder peak is somewhat lower. Interestingly, there are differences in the intensities of the composites with 1%, 2%, and 3% nanoclay between these two extremes.

The parameter changes between non-functionalized nano clay (NFNC) composites and functionalized composites with 1%, 2%, and 3% addition of nano clay powder are shown in figure 6. When comparing the functionalized nano clay powder (at 1%, 2%, and 3%), to its non-functionalized equivalent, a discernible variation in intensity is found. When compared to non-functionalized nanoclay, the intensity increases proportionately with the amount of nano clay powder utilised, usually by 10% to 12%. However, subsequent improvements demonstrate a diminishing trend, culminating in a 35% to 40% enhancement over the non-functionalized nanoclay composite.

In conclusion, it is showing that the functionalized nano clay composite exhibits more intensity than the non-functionalized one. This is explained by the fact that, in functionalized nano clay composites, the dispersion of the particles is uniform throughout the matrix, whereas in non-functionalized nano clay composites, it is uneven. When compared to the functionalized equivalent, this difference in dispersion results in a decrease in intensity.

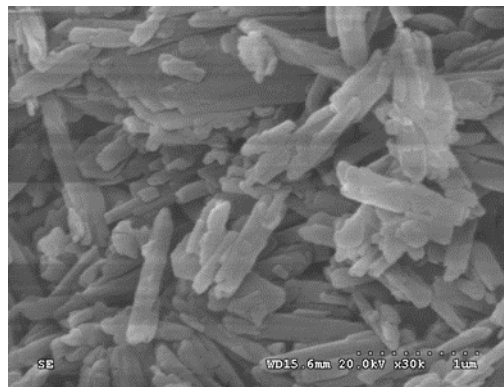


Figure 7: SEM photo of nanoclay (Hollow Nano Tubes)

An SEM image of the nanoclay's nanotubular structure is shown in Figure 7. The length-to-diameter ratio and typical diameter of ten randomly selected nanotubes were measured. The diameter ranges from 30 nm to 70 nm and the length/diameter ratio is in the range of 3×10^4 .

Wear test

A wear test was performed on a pin-on-disk configuration (DUCOM, TR-20-M26) to determine the nanoclay composites samples wear rate. Wear resistance, which is inversely related to wear rate, is a crucial measure for the composite's durability in this study. Two instruments were used to assess the wear rates of the clay powder reinforced epoxy composites: a tribometer and a surface profilometer. A load with the range of 5 to 25 N was applied on the specimens, which were rotated at 640 rpm, for 15 minutes. Fig 11 (a, b, c and d) shows the variation of wear rate with different ratios of fillers. When the filler ratio is 1%, 2% and 3%, the 2% wear rate becomes lower because clay particles oppose surface reduction of the composite. It is seen that the nano clay filled epoxies show good performance in wear resistance. Additionally, when the clay particles are liberated from the composite, they are tougher than the epoxy resin; their abrasiveness increases the composite wear rate.

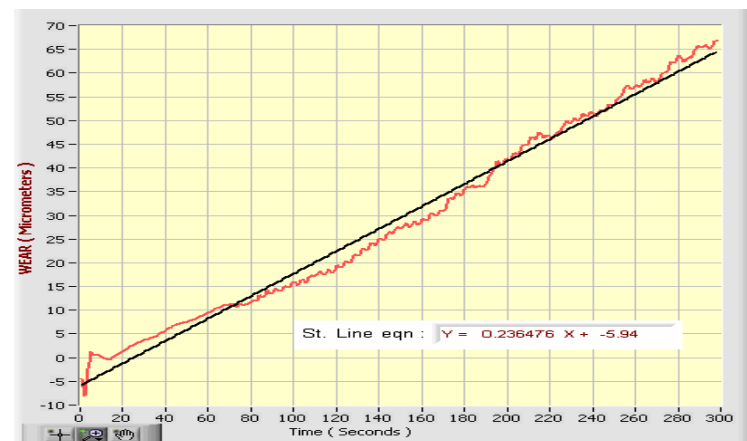


Figure 8: Wear of the pure samples at 25N and travel distance of 1.81km

Figure 8 depicts the obtained wear rate, modeled using a straight-line function $y = mx + c$, where "m" represents the wear rate. At a travel distance of 1.81 km and a weight of 25 N, the wear rate of the pure samples is found to be 0.237.

Under a load of 25N and a travel distance of 3.64 km, the wear rate of epoxy decreased from 0.237 to 0.042 nanometers per second in contrast to 2% reinforced HNT Nanoclay nanocomposites. Conversely, as Figure 10 illustrates, it increased to 0.158 nanometers per second when 3% HNT Nanoclay was added as reinforcement.

Notably, the wear rate is higher for pure epoxy composite, while 2% HNT Nanoclay reinforcement exhibits the lowest wear rate. The results of this experiment indicate that the wear rate and the nanocomposites' hardness are inversely related.

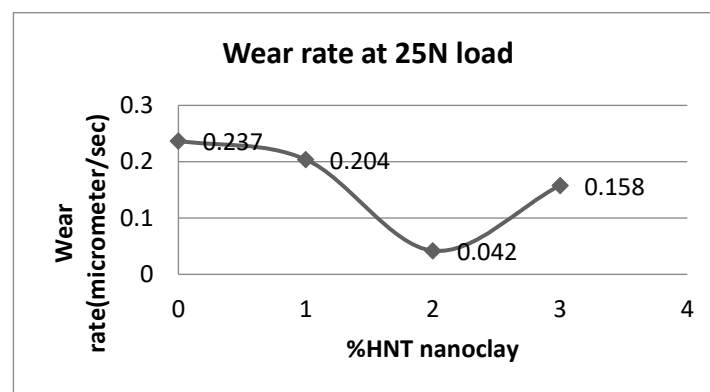


Figure 9: Wear rate by increasing the HNT Nano clay

Under a load of 25N and a travel distance of 3.64 km, the wear rate of epoxy decreased from 0.237 to 0.042 nanometers per second in contrast to 2% reinforced HNT Nanoclay nanocomposites. Conversely, as Figure 9 illustrates, it increased to 0.158 nanometers per second when 3% HNT Nanoclay was added as reinforcement. Notably, the wear rate is higher for pure epoxy composite, while 2% HNT Nanoclay reinforcement exhibits the lowest wear rate. The results of this experiment indicate that the wear rate and the nanocomposites' hardness are inversely related.

A 25N load was applied during the wear test. The wear rate is much reduced when 2% nanoclay particles are added, as seen in Fig. 10(d). The wear rate changes throughout loads of 5N, 15N, and 25N, as can be shown by comparing Figs. 10 (a), (b), (c), and (d). The lowest wear rate is consistently seen with 2% nanoclay particle addition. Based on these results, it is recommended to add 2% nanoclay particles, which is proportionate to the nanocomposites' hardness.

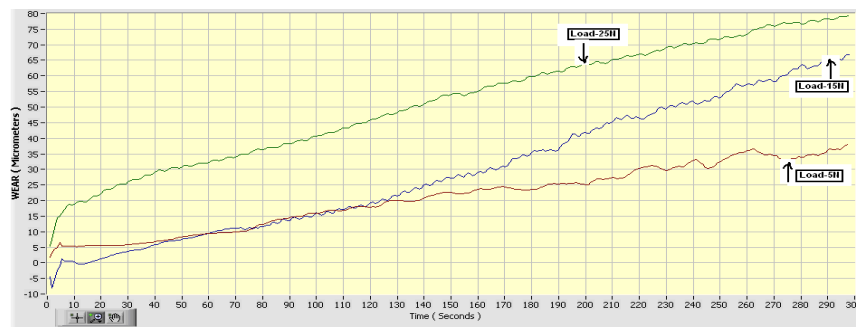


Figure 10: (a) Pure polymer composite wear under varying loads 5-25 N.

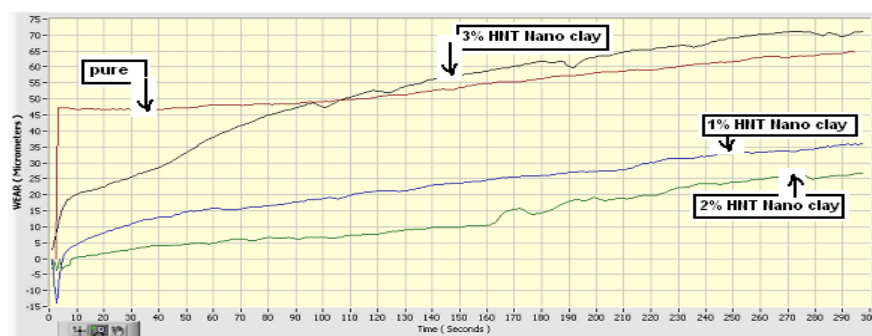


Figure 10: (b) Wear at load of 5 N for pure, 1%, 2%, and 3% HNT NC.

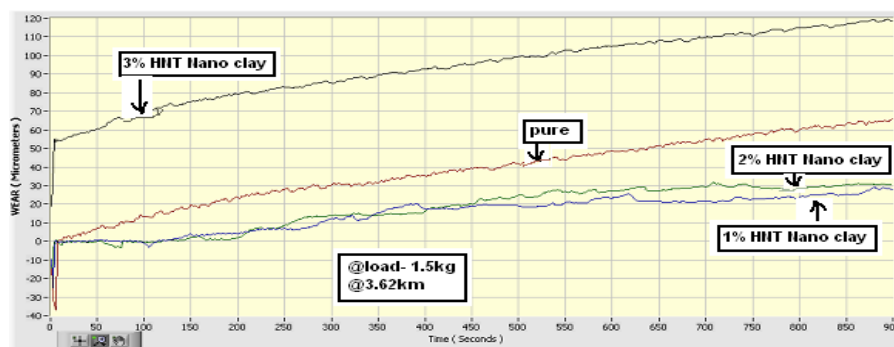


Figure 10: (c) Wear at load 5N and track distance 3.64km for pure, 1%HNT NC, 2%HNT NC and 3%HNT NC

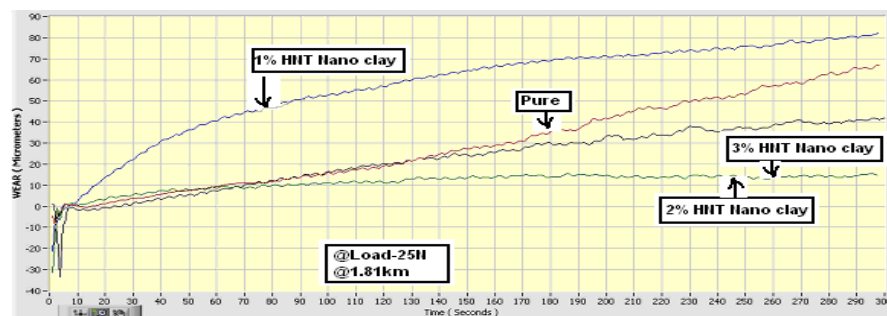


Figure 10: (d) Wear at load 25N and track distance 1.81km for pure, 1%HNT NC, 2%HNT NC and 3%HNT NC

4. Conclusion

Both functionalized and non-functionalized nano clay composites were characterized using X-ray diffraction. The development of nano composites led to the following conclusions based on the outcomes of the characterization of the nano clay particles.

Within the matrix, the non-functionalized composite shows insufficient dispersion of nano clay particles. Conversely, the chemically treated functionalized nano clay composite shows uniformly dispersed nano clay particles within the matrix. The non-functionalized nanoclay composite has a lower intensity than the functionalized nanoclay composite, according to the XRD data.

Under varied loads and durations, the wear test was conducted on samples of pure epoxy as well as 1%, 2%, and 3% nano clay composite materials. The findings indicate that the 2% nano clay composite shows the lowest wear rate among them, while pure epoxy shows a higher wear rate. Because the 2% nano clay composite is harder than pure epoxy and the 1%, 2%, and 3% nano clay composites, it wears down at a slower pace. It has been found that the hardness of nanocomposites and wear rate have an inverse connection.

Conflict of Interest:

The authors declare that they have no conflict of interest regarding the publication of this article. The research was conducted in the absence of any commercial or financial relationships that could be construed as a potential conflict of interest

References

- [1] Bandhu, D., Thakur, A., Purohit, R., Verma, R.K., Abhishek, K. Characterization & evaluation of Al7075 MMCs reinforced with ceramic particulates and influence of age hardening on their tensile behavior. *J. Mech. Sci. Technol.* 2018; 32: 3123–3128.
- [2] Sharma, S.K., Saxena, K.K., Malik, V., Mohammed, K.A., Prakash, C., Buddhi, D., Dixit, S. Significance of alloying elements on the mechanical characteristics of mg-based materials for biomedical applications. *Crystals.* 2022; 12: 1138.
- [3] Agarwal, K.M., Tyagi, R.K., Saxena, K.K. Deformation analysis of Al Alloy AA2024 through equal channel angular pressing for aircraft structures. *Adv. Mater. Process Technol.* 2020; 8: 828–842. <https://doi.org/10.1080/2374068X.2020.1834756>
- [4] Kumar, P.S.S., Allamraju, K.V. A review of natural fiber composites [Jute, Sisal, Kenaf]. *Mater.TodayProc.* 2019; 18: 2556–2562.
- [5] Portier, C., Pandelaere, K., Delaet, U., Vigh, T., Di Pretoro, G., De Beer, T., Vervaeet, C., Vanhoorne, V. Continuous twin screw granulation: a complex interplay between formulation properties, process settings and screw design. *Int. J. Pharm.* 2020; 576: 119004.
- [6] Awasthi, A., Saxena, K.K., Arun, V. Sustainable and smart metal forming manufacturing process. *Mater. Today Proc.* 2021; 44: 2069–2079.
- [7] Bhardwaj, A.R., Vaidya, A.M., Meshram, P.D., Bandhu, D. Machining behavior investigation of aluminium metal matrix composite reinforced with TiC particulates. *Int. J. Interact Des. Manuf.* 2023; 5: 1–15.
- [8] Yadav, P., Beniwal, G., Saxena, K.K. A review on pore and porosity in tissue engineering. *Mater. Today Proc.* 2021; 44: 2623–2628.
- [9] Zadafiya, K., Bandhu, D., Kumari, S., Chatterjee, S., Abhishek, K. Recent trends in drilling of carbon fiber reinforced polymers (CFRPs): a state-of-the-art review. *J. Manuf. Process.* 2021; 69: 47–68.
- [10] Bandari, S., Nyavanandi, D., Kallakunta, V.R., Janga, K.Y., Sarabu, S., Butreddy, A., Repka, M.A. Continuous twin screw granulation An advanced alternative granulation technology for use in the pharmaceutical industry. *Int. J. Pharm.* 2020; 8: 119–124.
- [11] Jha, P., Shaikshavali, G., Shankar, M.G., Ram, M.D.S., Bandhu, D., Saxena, K.K., Buddhi, D., Agrawal, M.K. A hybrid ensemble learning model for evaluating the surface roughness of AZ91 alloy during the end milling operation. *Surf. Rev. Lett.* 2022; 10: 89–93.

-
- [12] Kumari, S., Sonia, P., Singh, B., Abhishek, K., Saxena, K.K. Optimization of surface roughness in EDM of pure magnesium (Mg) using TLBO. *Mater. Today Proc.* 2020; 26: 2458–2461.
- [13] Agarwal, K.M., Tyagi, R.K., Saxena, V., Choubey, K.K. Mechanical behaviour of Aluminium Alloy AA6063 processed through ECAP with optimum die design parameters. *Adv. Mater. Process. Technol.* 2021; 9: 1901–1915.
- [14] Krishnaja, D., Cheepu, M., Venkateswarlu, D. A review of research progress on dissimilar laser weld-brazing of automotive applications. *IOP Conf. Ser. Mater. Sci. Eng.* 2018;10: 310-315 .
- [15] Agarwal, K.M., Tyagi, R.K., Saxena, K.K. Deformation analysis of Al Alloy AA2024 through equal channel angular pressing for aircraft structures. *Adv. Mater. Process Technol.* 2020; 8: 828–842.
- [16] Awasthi, A., Saxena, K.K., Arun, V. Sustainable and smart metal forming manufacturing process. *Mater. Today Proc.* 2021; 44: 2069–2079.
- [17] Sahai, N., Saxena, K.K., Gogoi, M.: Modelling and simulation for fabrication of 3D printed polymeric porous tissue scaffolds. *Adv. Mater. Process. Technol.* 2020; 6: 530–539.
- [18] Sathish, T., Kaliyaperumal, G., Velmurugan, G., Jose Arul, S., Melvin Victor, D.P., Nanthakumar, P. Investigation on augmentation of mechanical properties of AA6262 aluminium alloy composite with magnesium oxide and silicon carbide. *Mater. Today Proc.* 2021; 46: 4322–4325.
- [19] Jaffery, H.A., Sabri, M.F.M., Said, S.M., Hasan, S.W., Sajid, I.H., Nordin, N.I.M., Megat Hasnan, M.M.I., Shnawah, D.A., Moor- thy, C.V.: Electrochemical corrosion behavior of Sn-0.7Cu solder alloy with the addition of bismuth and iron. *J. Alloys Compd.* 2019; 810: 151925 2019.
- [20] Bhardwaj, A.R., Vaidya, A.M., Meshram, P.D., Bandhu, D. Machining behavior investigation of aluminium metal matrix composite reinforced with TiC particulates. *Int. J. Interact Des. Manuf.* 2023; 5: 1–15.
- [21] Mehta, A., Vasudev, H., Singh, S., Prakash, C., Saxena, K.K., Linul, E., Buddhi, D., Xu, J. Processing and advancements in the development of thermal barrier coatings: a review. *Coatings* 2022; 12: 13-18.
- [22] Kumari, S., Sonia, P., Singh, B., Abhishek, K., Saxena, K.K. Optimization of surface roughness in EDM of pure magnesium (Mg) using TLBO. *Mater. Today Proc.* 2020; 26: 2458–2461.
- [23] Agarwal, K.M., Tyagi, R.K., Saxena, V., Choubey, K.K. Mechanical behaviour of Aluminium Alloy AA6063 processed through ECAP with optimum die design parameters. *Adv. Mater. Process. Technol.* 2021; 9: 1901–1915.
- [24] Sahai, N., Saxena, K.K., Gogoi, M. Modelling and simulation for fabrication of 3D printed polymeric porous tissue scaffolds. *Adv. Mater. Process. Technol.* 2020; 6: 530–539.
- [25] Nagendra, J., Prasad, M.S.G. FDM process parameter optimization by taguchi technique for augmenting the mechanical properties of nylon-aramid composite used as filament material. *J. Inst. Eng. Ser.* 2020; 101: 313–322.